

In Vitro Activities of ER-119884 and E5700, Two Potent Squalene Synthase Inhibitors, against *Leishmania amazonensis*: Antiproliferative, Biochemical, and Ultrastructural Effects[∇]

Juliany Cola Fernandes Rodrigues,¹ Juan Luis Concepcion,² Carlos Rodrigues,³
Aura Caldera,³ Julio A. Urbina,^{3*} and Wanderley de Souza^{1*}

Laboratório de Ultraestrutura Celular Hertha Meyer, Instituto de Biofísica Carlos Chagas Filho, Universidade Federal do Rio de Janeiro, CCS, Bloco G, subsolo, Ilha do Fundão, Rio de Janeiro, RJ 21.941-902, Brazil¹; Laboratorio de Enzimología de Parasitos, Facultad de Ciencias, Universidad de los Andes, Merida, Venezuela²; and Laboratório de Química Biológica, Centro de Bioquímica y Biofísica, Instituto Venezolano de Investigaciones Científicas, Apartado 21827, Caracas 1020A, Venezuela³

Received 17 December 2007/Returned for modification 8 March 2008/Accepted 20 August 2008

ER-119884 and E5700, novel arylquinuclidine derivatives developed as cholesterol-lowering agents, were potent in vitro growth inhibitors of both proliferative stages of *Leishmania amazonensis*, the main causative agent of cutaneous leishmaniasis in South America, with the 50% inhibitory concentrations (IC₅₀s) being in the low-nanomolar to subnanomolar range. The compounds were very potent noncompetitive inhibitors of native *L. amazonensis* squalene synthase (SQS), with inhibition constants also being in the nanomolar to subnanomolar range. Growth inhibition was strictly associated with the depletion of the parasite's main endogenous sterols and the concomitant accumulation of exogenous cholesterol. Using electron microscopy, we identified the intracellular structures affected by the compounds. A large number of lipid inclusions displaying different shapes and electron densities were observed after treatment with both SQS inhibitors, and these inclusions were associated with an intense disorganization of the membrane that surrounds the cell body and flagellum, as well as the endoplasmic reticulum and the Golgi complex. Cells treated with ER-119884 but not those treated with E5700 had an altered cytoskeleton organization due to an abnormal distribution of tubulin, and many were arrested at cytokinesis. A prominent contractile vacuole and a phenotype typical of programmed cell death were frequently found in drug-treated cells. The selectivity of the drugs was demonstrated with the JC-1 mitochondrial fluorescent label and by trypan blue exclusion tests with macrophages, which showed that the IC₅₀s against the host cells were 4 to 5 orders of magnitude greater than those against the intracellular parasites. Taken together, our results show that ER-119884 and E5700 are unusually potent and selective inhibitors of the growth of *Leishmania amazonensis*, probably because of their inhibitory effects on de novo sterol biosynthesis at the level of SQS, but some of our observations indicate that ER-119884 may also interfere with other cellular processes.

Leishmaniasis comprises a group of infectious diseases caused by several species of *Leishmania* with three different clinical forms, visceral, cutaneous, and mucocutaneous. It is associated with significant rates of morbidity and mortality in many countries around the world and affects ca. 15 million people (21, 30, 53). *Leishmania amazonensis* is the species responsible for cutaneous leishmaniasis in South America, where the lesions are confined to the skin. However, in some individuals, infections can develop into diffuse leishmaniasis when the patient's immune system fails to react against the parasite (30), and it has also been reported that this parasite can cause visceral or post-kala-azar dermal leishmaniasis (1).

Currently, the mainstay of the chemotherapy employed for

the treatment of visceral and cutaneous/mucocutaneous leishmaniasis in Brazil remains pentavalent antimonials, such as pentostam and glucantime, which are very unsatisfactory due to their frequent toxic effects and the growing rates of resistance to the drugs in several parts of the world (11). Secondary treatments include pentamidine and amphotericin B, which are mainly employed in resistant cases when the antimonials fail (10). For visceral leishmaniasis, miltefosine (Impavido) has successfully been employed by the oral route in India (42), but a WHO report indicates that it is teratogenic and has a narrow chemotherapeutic window (17). Paromomycin and liposomal amphotericin B are other agents that may possibly be used against visceral leishmaniasis, and they are currently used to treat Indian patients living in regions where the resistance of the parasite to antimonials is widespread. On the other hand, for cutaneous leishmaniasis, new alternatives such as short courses of antimonial, topical paromomycin, and oral miltefosine have been developed; however, those studies are in progress in areas of endemicity, such as Guatemala and Colombia, and inconsistent results are being obtained between the different regions (3). Thus, there is a great necessity to develop new drugs that are efficacious, safe, and more accessible.

* Corresponding author. Mailing address for Wanderley de Souza: Laboratório de Ultraestrutura Celular Hertha Meyer, Instituto de Biofísica Carlos Chagas Filho, Universidade Federal do Rio de Janeiro, CCS, Bloco G, subsolo, Ilha do Fundão, Rio de Janeiro, RJ 21.941-902, Brazil. Phone: 55-21-25626581. Fax: 55-21-22602364. E-mail: wsouza@biof.ufrj.br. Mailing address for Julio A. Urbina: Laboratório de Química Biológica, Centro de Bioquímica y Biofísica, Instituto Venezolano de Investigaciones Científicas, Apartado 21827, Caracas 1020A, Venezuela. Phone and fax: (513) 321-2981. E-mail: jurbina@mac.com.

[∇] Published ahead of print on 2 September 2008.

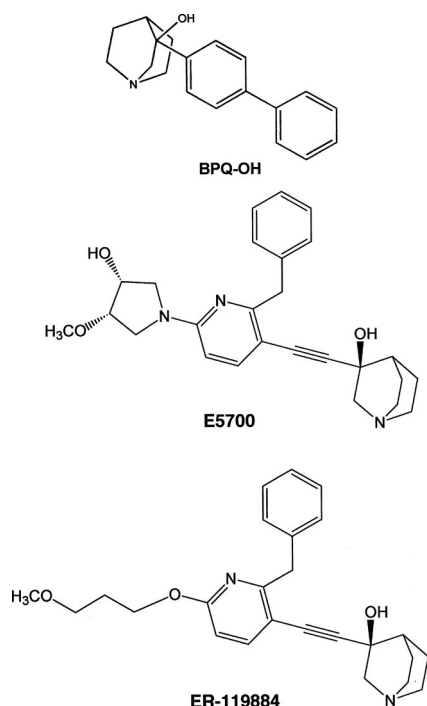


FIG. 1. Chemical structures of BPO-OH, E5700, and ER-119884.

Several studies have shown that the ergosterol biosynthesis pathway is a promising target in the development of a rational chemotherapeutic strategy against *Leishmania* and other trypanosomatids, because ergosterol is essential for the parasite's viability and is absent in mammalian cells (36, 47). Different classes of ergosterol biosynthesis inhibitors have been shown to be active against trypanosomatid parasites (4, 6, 9, 19, 23–27, 29, 35–39, 41, 45–49, 51, 52). One important enzyme of the sterol biosynthesis pathway is squalene synthase (SQS), which catalyzes the head-to-head condensation of two molecules of farnesyl pyrophosphate (FPP) to produce squalene (2). This is the first committed step in the sterol pathway, and its inhibition does not affect the biosynthesis of other essential isoprenoids (18). SQS has been under intense scrutiny with the aim of developing new cholesterol-lowering agents for humans. Previous work has demonstrated the effect of quinuclidine-based SQS inhibitors as cholesterol- and triglyceride-lowering agents in experimental studies with animals (5, 7, 33). On the other hand, several reports have described the potent and selective activity of the same class of compounds against parasites such as *Leishmania*, *Trypanosoma cruzi*, and *Toxoplasma gondii* (4, 6, 9, 26, 32, 39, 41, 48, 49). ER-119884 and E5700 (Fig. 1), two novel quinuclidine-based SQS inhibitors developed by Eisai Co. (Tokyo, Japan) as cholesterol- and triglyceride-lowering agents in humans, have recently been shown to be potent anti-*Trypanosoma cruzi* agents in vitro and in vivo, and their activities have been shown to be associated with a dramatic depletion of the parasite's endogenous sterols (48). In vivo studies with a murine model of acute Chagas' disease indicated that E5700 is able to provide full protection against death and to completely suppress the parasitemia, with no toxicity to the host (48). That study indicated that ER-119884

and E5700 potentially have activity against trypanosomatid parasites. On the other hand, these compounds were also active against *Toxoplasma gondii*, a parasite that does not synthesize endogenous sterols (32), probably indicating that another still unknown target(s) of arylquinuclidines is present in this parasite. In addition, there have been studies on the effects of 3-(biphenyl-4-yl)-3-hydroxyquinuclidine (3-biphenyl-4-yl-1-aza-bicyclo[2,2,2]-octan-3-ol; BPO-OH; Fig. 1), another potent SQS inhibitor, on the structures of *T. cruzi* (4) and *L. amazonensis* (39) cells; those studies showed that this inhibitor induces ultrastructural alterations in several subcellular organelles, including plasma and flagellar membranes, the endoplasmic reticulum, the Golgi complex, and the mitochondrion. Both studies also described the appearance of typical features of programmed cell death in drug-treated cells.

In the present study, we investigated the antiproliferative, biochemical, and ultrastructural effects of ER-119884 and E5700 on *Leishmania amazonensis* and found that they are among the agents with the most potent and selective activities against this parasite ever tested.

MATERIALS AND METHODS

Parasites. Two strains of *Leishmania amazonensis* were used in this study: strain NR, previously classified as *Leishmania mexicana amazonensis* but now included in the species *L. amazonensis* (28), and strain MHOM/BR/75/Josefa (strain Josefa), which was isolated from a patient with diffuse cutaneous leishmaniasis by C. A. Cuba-Cuba (Universidade de Brasília, Brasília, Brazil). Both strains have been maintained in BALB/c mice by footpad inoculation and, in the case of promastigotes, axenically cultured in LIT-B medium (49) for strain NR and in Warren's medium (brain heart infusion plus hemin and folic acid) for strain Josefa; the media were supplemented with 10% fetal bovine serum, and the cells were grown statically at 28°C. Infective promastigotes of strain Josefa were used to obtain intracellular amastigotes in macrophage cultures.

Drugs. BPO-OH was synthesized and purified as described by Brown et al. (5), with slight modifications. ER-119884 {(3R)-3-[[2-benzyl-6-(3-methoxypropyloxy)pyridin-3-yl]ethynyl]quinuclidin-3-ol} and E5700 {(3R)-3-[[2-benzyl-6-[3R,4S]-3-hydroxy-4-methoxyproline-1-yl]pyridin-3-yl]ethynyl]quinuclidin-3-ol monohydrate} were provided by Tsukuba Research Laboratories, Eisai Co. For the in vitro studies, the compounds were dissolved in dimethyl sulfoxide (DMSO), the final concentrations of DMSO in the cultures did not exceed 0.1% (vol/vol) and had no effect on cell proliferation. Stock solutions were stored at 0 to 4°C.

In vitro activities of ER-119884 and E5700. Growth experiments with promastigotes of both strains of *L. amazonensis* were initiated with 2.0×10^6 parasites/ml, and the inhibitors were added at different concentrations from concentrated stock solutions in DMSO after 24 h of growth. Cell densities were evaluated daily in a hemocytometer and by turbidimetry (600 nm) for 5 days. To evaluate the effects of the inhibitors on the intracellular amastigote forms of *L. amazonensis*, peritoneal macrophages from BALB/c mice were harvested by washing them with RPMI medium (Gibco), plating them in 24-well tissue culture chamber slides, and allowing them to adhere to the slides for 24 h at 37°C in 5% CO₂. Adherent macrophages were infected with metacyclic promastigotes at a macrophage-to-parasite ratio of 1:10 at 35°C for 2 h. After this time, the noningested parasites were removed by washing and the infected cultures were incubated for 24 h in RPMI without the inhibitors. ER-119884 and E5700 were added at different concentrations after 24 h of interaction, when the number of amastigotes per macrophage was in the range of two to four, and fresh medium with inhibitors was added daily for 4 days. The cultures were fixed with 4% paraformaldehyde in saline phosphate buffer (pH 7.2) and stained with Giemsa for 30 min. The percentage of infected cells was determined by light microscopy. Association indexes (mean number of parasites internalized multiplied by the percentage of infected macrophages divided by the total number of macrophages) were determined. The 50% inhibitory concentrations (IC₅₀s) were calculated with the SigmaPlot (version 8) program. The results are expressed as the means of three independent experiments.

Tests of viability in macrophages. To evaluate the cytotoxicities of ER-119884 and E5700 against macrophage cultures, cells were incubated with the indicated concentrations of the drugs for 96 h, and exclusion tests with 0.1% trypan blue were carried out for 5 min. The percentages of dead and alive cells were deter-

mined after 300 macrophages in randomly selected fields were counted by light microscopy. In addition, the mitochondrial membrane potential ($\Delta\Psi$) of control macrophages as well as that of cells treated with different concentrations of E5700 and ER-119884 (5 to 500 nM) was determined with the potentiometric probe JC-1. JC-1 is a cationic mitochondrial vital dye that is lipophilic and that becomes concentrated in the mitochondria in response to $\Delta\Psi$. The dye exists as a monomer at low concentrations, where the emission is 530 nm (green fluorescence), but at higher concentrations it forms J-aggregates, where the emission is 590 nm (red fluorescence). Thus, the fluorescence of JC-1 is considered an indicator of an energized mitochondrial state. Control and treated macrophages were incubated for 30 min with 10 μM JC-1 at 37°C, washed with phosphate-buffered saline (PBS; pH 7.2), and observed under a Zeiss Axioplan epifluorescence microscope. The fluorescence was collected with a 500- to 550-nm band-pass filter for monomer detection and a 560-nm long-pass filter for aggregate detection, and the images were recorded with a C5810 Hamamatsu camera.

Isolation and purification of SQS from *Leishmania amazonensis* promastigotes. The purification of native glycosomal and microsomal SQS from *Leishmania amazonensis* NR promastigotes was carried out as described by Urbina et al. (49). Briefly, cells which had been grown in LIT medium were harvested, washed in PBS, homogenized by gentle grinding with silicon carbide, and fractionated by sequential differential and isopycnic centrifugation. Subcellular fractions were identified by their densities and marker enzymes, as described in detail by Concepcion et al. (8).

Assay of SQS activity. SQS activity was measured by the radioactive spot-wash assay developed by Tait (43).

Kinetic calculations. Initial velocity (V) data were obtained as a function of the substrate concentration ($[S]$) and inhibitor concentration ($[I]$) and by keeping the cosubstrate concentration at saturating levels, and the data were fitted to the following equation (44): $1/V = \{(1 + [I]/K_{ii})/V_m\} + \{(1 + [I]/K_{is})K_m/V_m[S]\}$, where K_m and V_m are the apparent Michaelis-Menten constant and the maximal velocity, respectively, and where $K_{ii} = ([E'S][I])/[E'SI]$ and $K_{is} = ([E']^2[I])/[E']$, where $[E']$ and $[E'S]$ are the concentrations of the free enzyme and the enzyme-substrate complex, respectively, in the presence of fixed concentrations of the cosubstrate and cofactors. Kinetic constants were estimated by nonlinear regression analysis with the SigmaPlot (version 8) software package.

Studies of lipid composition. For the analysis of the effects of the drugs on the lipid composition of the promastigotes, total lipids were extracted from control and drug-treated *Leishmania amazonensis* NR promastigotes and were fractionated into neutral and polar lipid fractions by silicic acid column chromatography and gas-liquid chromatography (45, 46). The neutral lipid fractions were first analyzed by thin-layer chromatography (on Merck 5721 silica gel plates with heptane-isopropyl ether-glacial acetic acid [60:40:4] as the developing solvent) and conventional gas-liquid chromatography (isothermal separation in a 4-m glass column packed with 3% OV-1 on Chromosorb 100/200 mesh, with nitrogen as the carrier gas at 24 ml/min, and with flame ionization detection in a Varian 3700 gas chromatograph). For quantitative analysis and structural assignments, the neutral lipids were separated in a capillary high-resolution column (an Ultra-2 column of 25 m by 0.20 mm [inner diameter] with 5% phenyl-methylsiloxane and a film thickness of 0.33 μm) in a Hewlett-Packard 6890 Plus gas chromatograph equipped with an HP5973A mass-sensitive detector. The lipids were dissolved in chloroform and injected; the column was kept at 50°C for 1 min, and then the temperature was increased to 270°C at a rate of 25°C \cdot min⁻¹ and finally to 300°C at a rate of 1°C \cdot min⁻¹. The flow rate of the carrier gas (He) was kept constant at 0.5 ml \cdot min⁻¹. The injector temperature was 250°C, and the detector was kept at 280°C.

Fluorescence microscopy. Control and treated parasite cells were fixed for 30 min at room temperature in 4% paraformaldehyde in 0.1 M phosphate buffer (pH 7.2) and allowed to adhere to coverslips. Two different fluorescent labeling procedures were used in this study: one with 4',6'-diamidino-2-phenylindole (DAPI) to label the DNA and the other with Nile red to label the lipid bodies. For DAPI fluorescence, the parasites that adhered were permeabilized with 1% Triton X-100 in 0.1 M phosphate buffer (pH 7.2) for 5 min and incubated in a DAPI solution for 15 min. In the case of Nile Red fluorescence, the adherent parasites were incubated in 10 $\mu\text{g}/\text{ml}$ Nile Red for 30 min. After the incubations, the coverslips were mounted in glass slides with *n*-propyl-galate, sealed, and observed under a Zeiss Axioplan epifluorescence microscope equipped with DAPI and rhodamine filters. The images were recorded with a C5810 Hamamatsu camera.

Immunofluorescence microscopy. Two different methodologies were used to observe changes in the cytoskeletons of the treated cells. By the first methodology, control and parasites treated with BPQ-OH, ER-119884, and E5700 were fixed and permeabilized with absolute methanol for 10 min at -20°C. By the second methodology, parasites were fixed for 30 min at room temperature in 4%

paraformaldehyde in 0.1 M PHEM buffer (pH 7.2), allowed to adhere to coverslips, and permeabilized with 1% Triton X-100 in 0.1 M PHEM (25 mM MgCl₂, 35 mM KCl, 5 mM EGTA, 10 mM HEPES, 30 mM PIPES) buffer (pH 7.2) for 5 min. After fixation and permeabilization, the samples were blocked for 1 h in a solution of PBS (pH 8.0) containing 1.5% albumin and 0.25% fish gelatin and were incubated for 1 h with the TAT1 monoclonal antibody against α -tubulin (diluted 1:1 in a blockade buffer). Next, the samples were incubated with a secondary antibody, anti-mouse Alexa 488 (diluted 1:400). The coverslips were mounted in glass slides with *n*-propyl-galate, sealed, and observed under a Zeiss Axioplan epifluorescence microscope equipped with a fluorescein filter set. The images were recorded with a C5810 Hamamatsu camera.

Electron microscopy. Control and treated parasite cells were fixed for 24 h at 4°C in 2.5% glutaraldehyde in 0.1 M cacodylate buffer (pH 7.2). After fixation, the cells were postfixed for 30 min in a solution containing 1% OsO₄ and 1.25% potassium ferrocyanide solution in 0.1 M cacodylate buffer, washed in the same buffer, dehydrated in acetone, and embedded in Epon. Ultrathin sections were stained with uranyl acetate and lead citrate and were observed under a Jeol 1200 electron microscope.

RESULTS

In vitro antiproliferative effects of E5700 and ER-119884 on *Leishmania amazonensis*. E5700 and ER-119884 were potent antiproliferative agents against *Leishmania amazonensis* NR promastigotes, with MICs of 30 and 10 nM, respectively (Fig. 2). Very similar activities were observed against strain Josefa, with MICs of 50 and 10 nM and IC₅₀s of 6.7 and 0.92 nM for E5700 and ER-119884, respectively, after 96 h of incubation (Table 1 and data not shown). The two compounds were even more potent against clinically relevant intracellular amastigotes of strain Josefa cultivated in murine peritoneal macrophages, with IC₅₀s of 2.0 and 0.5 nM, respectively, after 96 h of contact with the drugs (Fig. 3 and Table 1) and with no detectable effects against the host cells. The mitochondrial $\Delta\Psi$ s of control and treated macrophage monolayers were determined by JC-1 fluorescence. The macrophages were treated for 4 days with concentrations that varied from 5 nM to 500 nM, concentrations 1,000- and 250-fold greater than the IC₅₀s obtained for ER-119884 and E5700, respectively. No difference in the intensity of the dye's red fluorescence between control and treated cells (Fig. 4A to F) was detected at any of the concentrations tested, indicating that the mitochondrial $\Delta\Psi$ s and, thus, the cells' viability were not compromised by the drug treatment. Differential interference contrast (DIC) microscopy also indicated that the macrophages were intact (Fig. 4A, C, and E). Furthermore, trypan blue exclusion tests were carried out with noninfected macrophages incubated with the drugs at up to 5 mM (the solubility limit) for 96 h. We obtained (Fig. 4G and H) IC₅₀s of 51.1 μM and 51.8 μM for ER-119884 and E5700, respectively, which were 100,000- and 25,000-fold greater than the corresponding IC₅₀s against the intracellular amastigotes. As reported in previous studies (38, 49), the final DMSO concentration in the cultures (0.1%) did not interfere with parasite growth or morphology.

Effects of E5700 and ER-119884 on *Leishmania amazonensis* SQS. As was found in a previous study (49), SQS has a dual localization in *Leishmania amazonensis* NR promastigotes: the glycosomes and the microsomes. E5700 and ER-119884 were very potent inhibitors of both enzyme isoforms, with IC₅₀s in the low-nanomolar or subnanomolar range in the absence or presence of 20 μM inorganic pyrophosphate, respectively (Table 2). Detailed kinetic studies demonstrated that these compounds were mixed or noncompetitive inhibitors of the enzyme

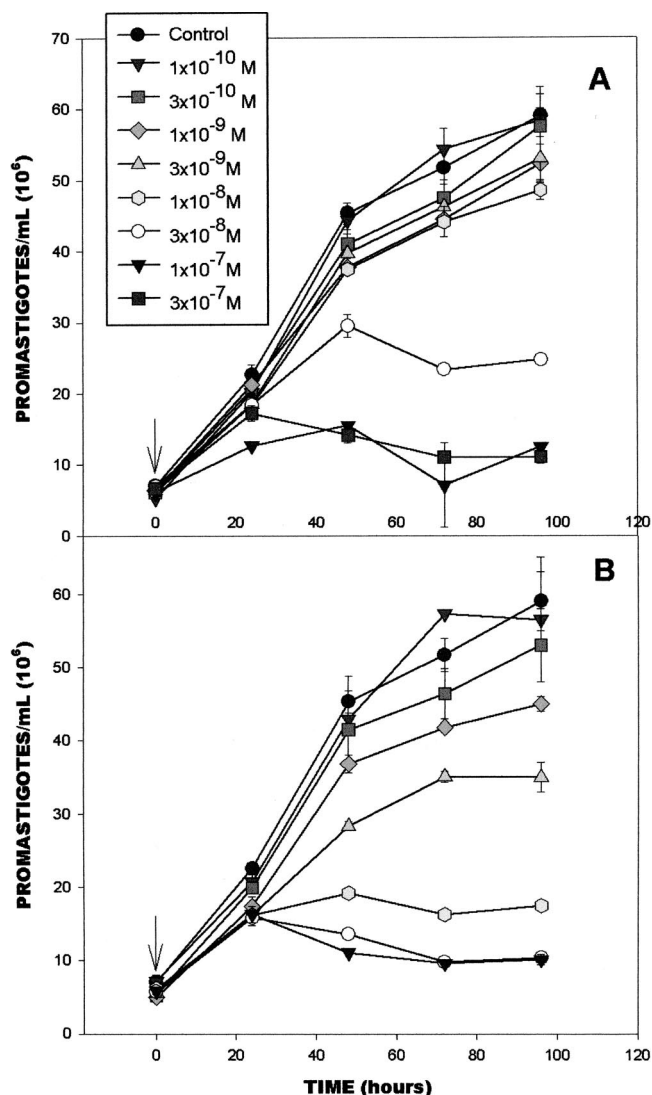


FIG. 2. Effects of E5700 (A) and ER-119884 (B) on the proliferation of *Leishmania amazonensis* NR promastigotes. Promastigotes were cultured statically in LIT-B medium at 28°C, as described in Materials and Methods. The arrows indicate the time of addition of the drug at the indicated concentrations. The experiments were carried out in triplicate, and each bar represents 1 standard deviation.

(Fig. 5 and 6, Table 3, and results not shown), with the K_{ii} and K_{is} values again being in the low-nanomolar to subnanomolar range.

Effects of E5700 and ER-119884 on *Leishmania amazonensis* free sterol composition. Consistent with their inhibitory actions on the parasite’s SQS, incubation of *Leishmania amazonensis* promastigotes with E5700 or ER-119884 induced a dose-dependent reduction of the relative levels of the main endogenous sterols, episterol and 5-dehydroepisterol, with no accumulation of sterol precursors, consistent with a blockade of de novo sterol biosynthesis at the level of SQS (Table 4). Depletion of the parasite’s endogenous sterols was associated with growth inhibition (Fig. 2 and Table 4). However, full growth arrest and a loss of cell viability arrest took place at concentrations of the drugs below those required for the com-

TABLE 1. Antiproliferative effects of E5700 and ER-119884 against promastigotes and intracellular amastigotes of *Leishmania amazonensis* Josefa^a

Stage	Incubation time (h)	IC ₅₀ (nM)	
		E5700	ER-119884
Promastigotes	72	14.7	1.7
	96	6.7	0.9
Intracellular amastigotes	72	4	0.9
	96	2	0.5

^a For details on the growth assays, see Materials and Methods.

plete depletion of the endogenous sterols (with exogenous cholesterol remaining the sole sterol in treated cells; Fig. 2 and Table 4).

Effects on tubulin cytoskeleton. Immunofluorescence microscopy was used to investigate the effects of the SQS inhibitors on the parasite’s cytoskeleton, constituted mainly by tubulin. Figure 7A and B shows DIC and fluorescence microscopic images for control parasites, which displayed a normal shape and labeling after initial incubation in the presence of antitubulin antibody and subsequent incubation with a secondary antibody conjugated to Alexa 488. Changes in the shape and cytoskeleton were observed after treatment with ER-

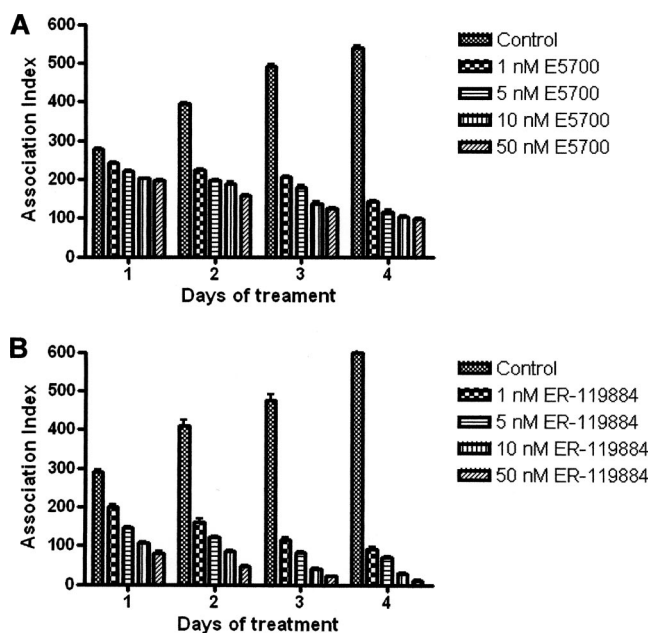


FIG. 3. Effects of E5700 (A) and ER-119884 (B) on the proliferation of *Leishmania amazonensis* intracellular amastigotes. Macrophage monolayers were first infected with metacyclic promastigotes for 24 h, and after that the different concentrations of E5700 and ER-119884 were added for 4 days. See Materials and Methods for details about the assays with the intracellular amastigotes. Experiments were carried out in triplicate, and each bar represents the standard deviation. Association indexes are the mean number of parasites internalized multiplied by the percentage of infected macrophages divided by the total number of macrophages. The Student test was calculated for data for each day and concentration, always in comparison with the results for the control, and P was <0.001 for all parameters.

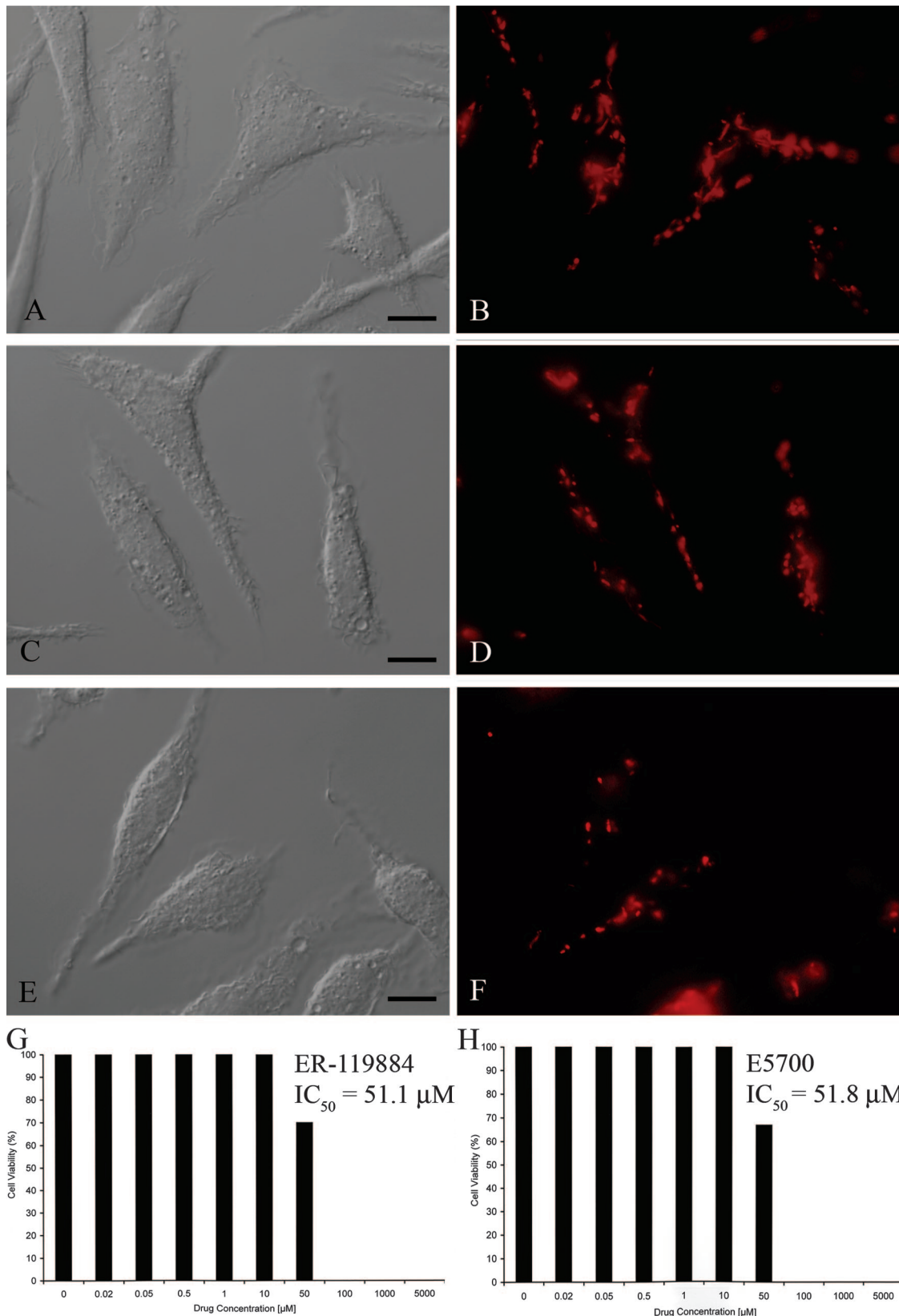


FIG. 4. DIC microscopy (left panels) and fluorescence microscopy with JC-1, a mitochondrial fluorescent dye (right panels), after 4 days treatment of macrophage cultures with 500 nM ER-119884 and E5700. (A and B) Macrophage control, without any treatment, showing the red fluorescence of the J-aggregate, which indicates that the mitochondria are intact; (C to F) macrophages treated with 500 nM ER-119884 (C and D) and E5700 (E and F) for 4 days, showing the same pattern of red fluorescence of the J-aggregate observed in the control macrophages, which also indicates that both SQS inhibitors do not affect the mitochondrial $\Delta\Psi$; (G and H) percentage of viable cells after treatment of macrophages with E5700 (G) and ER-119884 (H) for 96 h; the concentration given in each panel corresponds to the IC₅₀ of the compound. Bars, 5 μm.

TABLE 2. Inhibitory activities of E5700 and ER-119884 on SQS from *Leishmania amazonensis* NR promastigotes^a

Compound	IC ₅₀ (nM) without PP _i /IC ₅₀ (nM) with 20 μM PP _i	
	Glycosomal SQS	Microsomal or mitochondrial SQS
E5700	6.4/0.47	5.5/0.53
ER-119884	6.9/1.3	14.8/3.3

^a Highly purified glycosomes and microsomal or mitochondrial vesicles were obtained from cell homogenates prepared by grinding with silicon carbide, followed by differential and isopycnic centrifugation, as described elsewhere (8). SQS was assayed as described by Tait (43) in the presence of 0.1% Triton X-100, 20 μM FPP, and 1 mM NADPH.

119884 and BPQ-OH near their MICs (Fig. 7C to F) but not with E5700 up to its MIC (50 nM; data not shown). After fixation and permeabilization with methanol, fluorescence images (Fig. 7D and F) showed the formation of large tubulin clusters (white arrowheads) in treated parasites that was not seen in untreated cells and that probably resulted from the depolymerization of the tubulin dimers. This change in cytoskeleton was accompanied by an important change in the shape of the parasite cells, as observed in the DIC microscopic images (Fig. 7C and E). When the parasites were fixed with paraformaldehyde and permeabilized with Triton X-100, we also observed changes in the labeling of the tubulin, indicating that the clusters seen after methanol incubation were not an artifact of the extraction step but were a consequence of the treatment with the SQS inhibitors (Fig. 7G and H). These

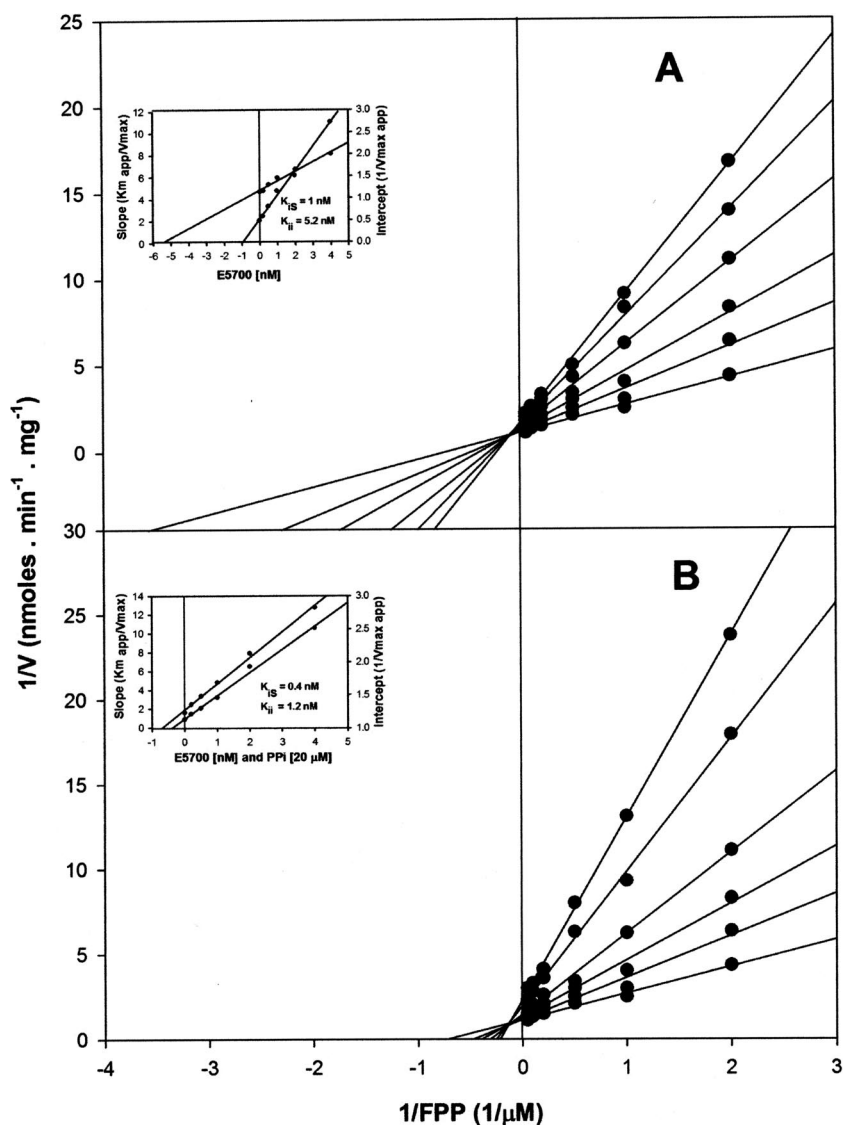


FIG. 5. Kinetics of *L. amazonensis* glycosomal SQS inhibition by E5700. Double-reciprocal plots of the enzyme activity as a function of various concentrations of FPP in the presence of 1 mM of the cosubstrate NADPH and the indicated concentrations of E5700 in the absence (A) or presence (B) of 20 μM PP_i are presented. (Insets) Secondary plots of the intercepts as a function of E5700 (app, apparent). SQS activity was measured in the presence of 0.1% Triton X-100, as described by Tait (43).

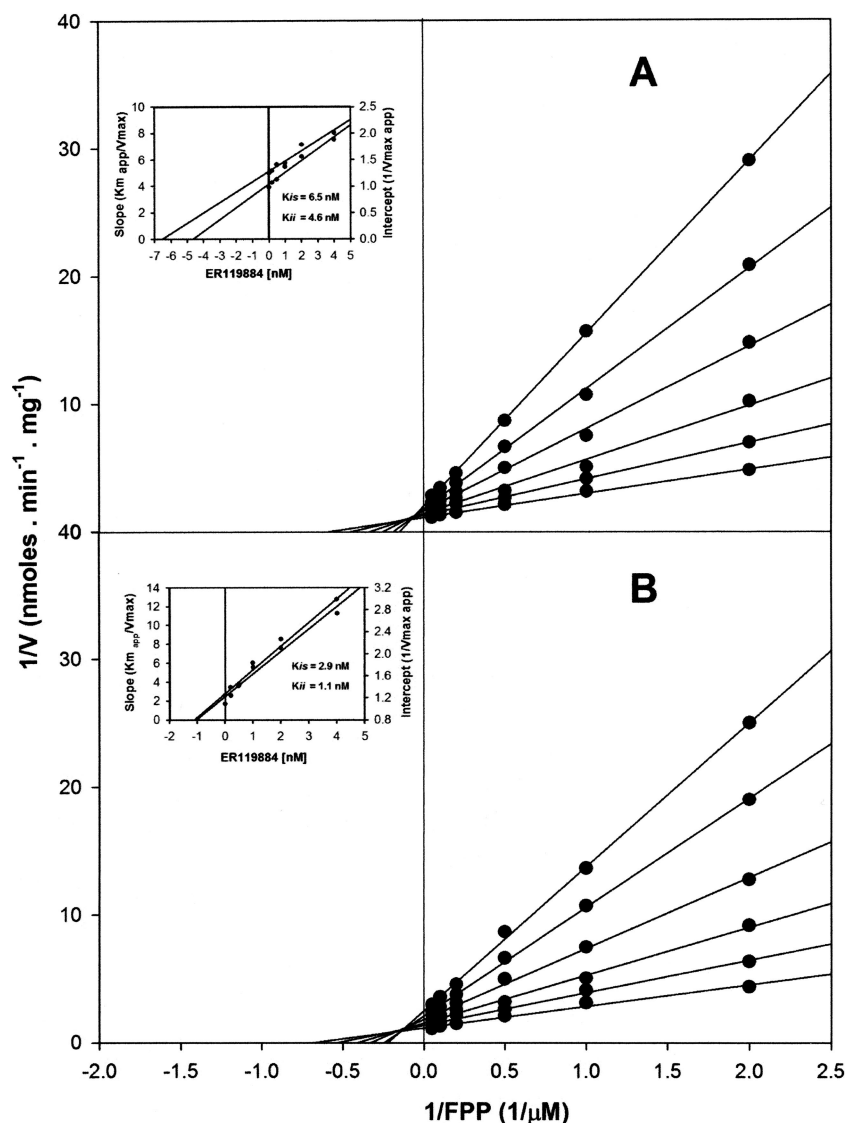


FIG. 6. Kinetics of *L. amazonensis* glycosomal SQS inhibition by ER-119884. Double-reciprocal plots of the enzyme activity as a function of various concentrations of FPP in the presence of 1 mM of the cosubstrate NADPH and the indicated concentrations of ER-119884 in the absence (A) or presence (B) of 20 μM PP_i are presented. (Insets) Secondary plots of the slopes as a function of ER-119884 (app, apparent). SQS activity was measured in the presence of 0.1% Triton X-100, as described by Tait (43).

changes in shape and in the organization of the cytoskeleton were observed in 60 to 80% of the treated cells.

Effects on cell cycle. Fluorescence microscopy of cells stained with DAPI to label the nucleus and kinetoplast revealed changes in the cell cycle in a subpopulation of cells

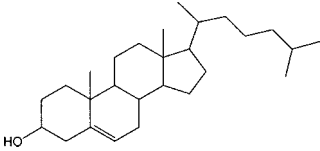
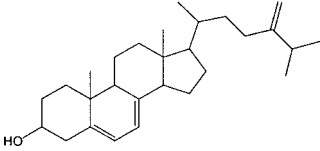
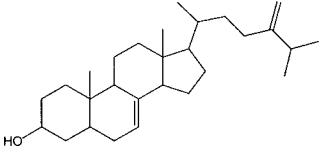
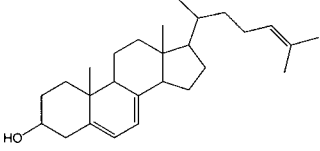
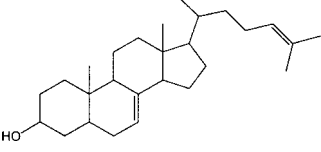
treated with ER-119884 (Fig. 8A to D), but these changes were absent in parasites treated with E5700 at concentrations up to its MIC (data not shown). Figure 8A shows control parasites after 48 h of culture presenting normal numbers of flagella (black arrow), kinetoplasts (white arrow), and nuclei (arrow-

TABLE 3. Inhibition kinetic constants for E5700 and ER-119884 on SQS from *Leishmania amazonensis* NR promastigotes^a

Enzyme source	K_i (nM) without PP_i / K_i (nM) with 20 μM PP_i				Inhibition type without PP_i /with 20 μM PP_i	
	K_{ii}		K_{is}		E5700	ER-119884
	E5700	ER-119884	E5700	ER-119884		
Glycosomes	5.2/1.2	4.6/1.1	1.0/0.4	6.5/2.9	Mixed/mixed	Noncompetitive/mixed
Microsomes	1.2/1.2	4.3/3.2	4.0/0.9	5.5/1.1	Mixed/noncompetitive	Noncompetitive/mixed

^a Highly purified glycosomes or microsomal vesicles were obtained from cell homogenates by grinding with silicon carbide, followed by differential and isopycnic centrifugation, as described elsewhere (8). SQS was assayed as described by Tait (43) in the presence of 0.1% Triton X-100.

TABLE 4. Effects of E5700 and ER-119884 on free sterol compositions of *Leishmania amazonensis* NR promastigotes^a

Compound	Molecular structure	Composition (mass %)						
		Control	E5700 10 nM	E5700 30 nM	E5700 50 nM	ER- 119884 3 nM	ER- 119884 10 nM	ER- 119884 30 nM
Exogenous cholesterol		11.7	21.4	58.1	>99	44.0	68.5	>99
Endogenous 14-desmethyl:								
Ergosta-5,7,24(24 ¹)-trien-3 β -ol (5-dehydroepisterol)		61.6	53.1	28.8	ND	36.8	17.3	ND
Ergosta-7,24(24 ¹)-dien-3 β -ol (episterol)		19.4	22.5	13.1	ND	19.2	14.2	ND
Cholesta-5,7,24-trien-3 β -ol		3.7	ND	ND	ND	ND	ND	ND
Cholesta-7,24-dien-3 β -ol		3.6	3.0	ND	ND	ND	ND	ND

^a Sterols were extracted from cells exposed to the indicated drug concentration for 96 h; they were separated from polar lipids by silicic acid column chromatography and were analyzed by quantitative capillary gas-liquid chromatography and mass spectrometry. ND, not detected.

head). After 24 h of treatment, about 5% of the parasites with several abnormalities in these structures were observed: Fig. 8B shows a parasite treated with 50 nM ER-119884 with four flagella (black arrows) but only one kinetoplast (white arrow) and one nucleus (arrowhead). After 48 h of treatment with 10 nM ER-119884 (Fig. 8C), parasites with three flagella (black arrows) and three nuclei (arrowheads) but only two kinetoplasts (black arrow) were found, indicating serious interference of ER-119884 with cell cycle progression, whereas after 72 h of treatment (Fig. 8D), some treated parasites presented abnormal shapes and up to four kinetoplasts (white arrows) and one nucleus (arrowhead). The presence of these aberrant phenotypes in association with altered cell cycles was quantified (Fig. 9A to C). After 48 and 72 h of treatment, the number of altered cells increased, with about 20% of the parasites exhibiting gross abnormalities.

Presence of lipid droplets. Fluorescence microscopy of control and treated parasites stained with Nile Red was carried out to visualize the possible accumulation of lipid droplets in the cytoplasm induced by the treatment with the SQS inhibitors. Figure 10A shows that the control parasites did not present

lipid droplets in the cytoplasm. After treatment with ER-119884 at 10 nM for 24 h, many lipid droplets were observed (Fig. 10B and C). Such lipid droplets were not seen in E5700-treated cells (data not shown).

Ultrastructural effects. Several changes in the ultrastructure of parasite cells treated with the SQS inhibitors were observed by transmission electron microscopy. Figure 11A shows a control promastigote form of *L. amazonensis* with a normal morphology. One important change took place in cells treated with either ER-119884 or E5700, in which the plasma membrane and flagellar membrane presented severe alterations, as seen in Fig. 11B and C (arrowheads). Similar changes were observed in intracellular membranes after treatment with ER-119884 at low concentrations and with short incubation times (10 nM for 24 h), when organelles such as the endoplasmic reticulum also had dramatic alterations (Fig. 11D, arrows) and the Golgi complex displayed dilated cisternae (Fig. 11E, big arrow). Treated parasites also showed lipid accumulation in the cytoplasm (Fig. 12A, arrow), and in some cases the lipid accumulation appeared to be surrounded by a membrane profile, probably the cisternae of the endoplasmic reticulum (Fig.

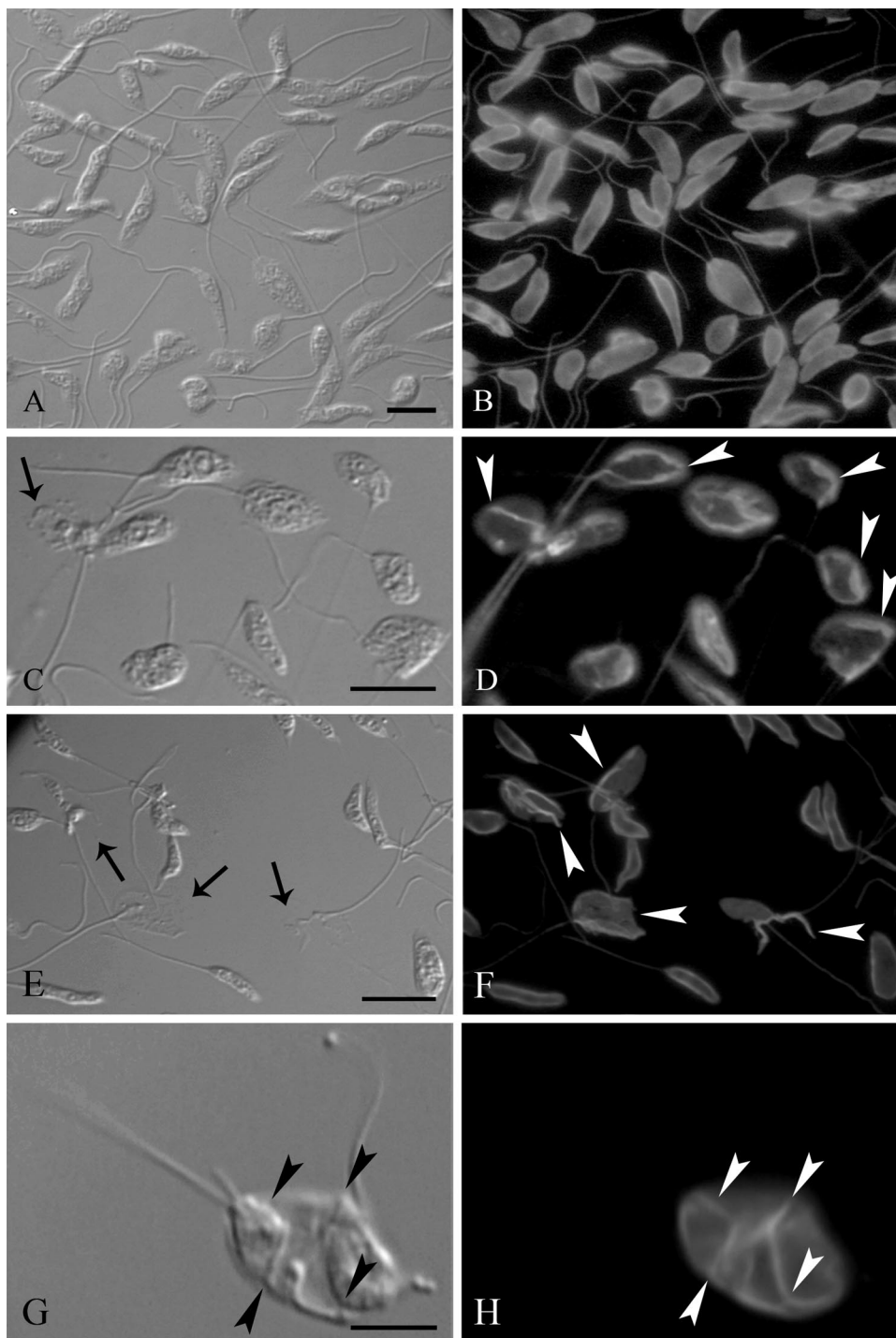


FIG. 7. DIC microscopy (left panels) and immunofluorescence microscopy (right panels) of promastigote forms of *Leishmania amazonensis* control cells (A and B), cells treated with 5 nM ER-119884 for 24 h (C and D), and cells treated with 1 μ M BPO-OH for 24 h (E and F). The labeling corresponds to the cytoskeleton constituted mainly by tubulin, which is revealed here by use of a secondary antibody, anti-mouse Alexa 488. Black arrows point to the cell body, and white arrowheads point to the accumulated tubulin that could be visualized after incubation with the SQS inhibitors. (A and B) General overview of control promastigotes presenting normal labeling in the subpellicular microtubules. Note in the DIC microscopy image that the parasites have the characteristic shape of the promastigotes. (C and D) After treatment with ER-119884, the parasites appeared to be swelled, as observed by DIC microscopy, and the labeling pattern for tubulin changed completely, with tubulin appearing as clusters that accumulated in the cytoplasm (white arrowheads). (E and F) Parasites treated with BPO-OH presenting the same alteration described for panels C and D. (G and H) The same labeling pattern for tubulin observed in panels C and D was observed in paraformaldehyde- and Triton X-100-treated cells. In the DIC microscopy image, it was possible to observe alterations in the membrane structure (black arrowheads) that correspond to the labeling for the tubulin observed by the fluorescence microscopy (white arrowheads). Black arrows point to regions of the cell bodies where the plasma membrane was completely extracted after treatment with methanol. Bars, 5 μ m.

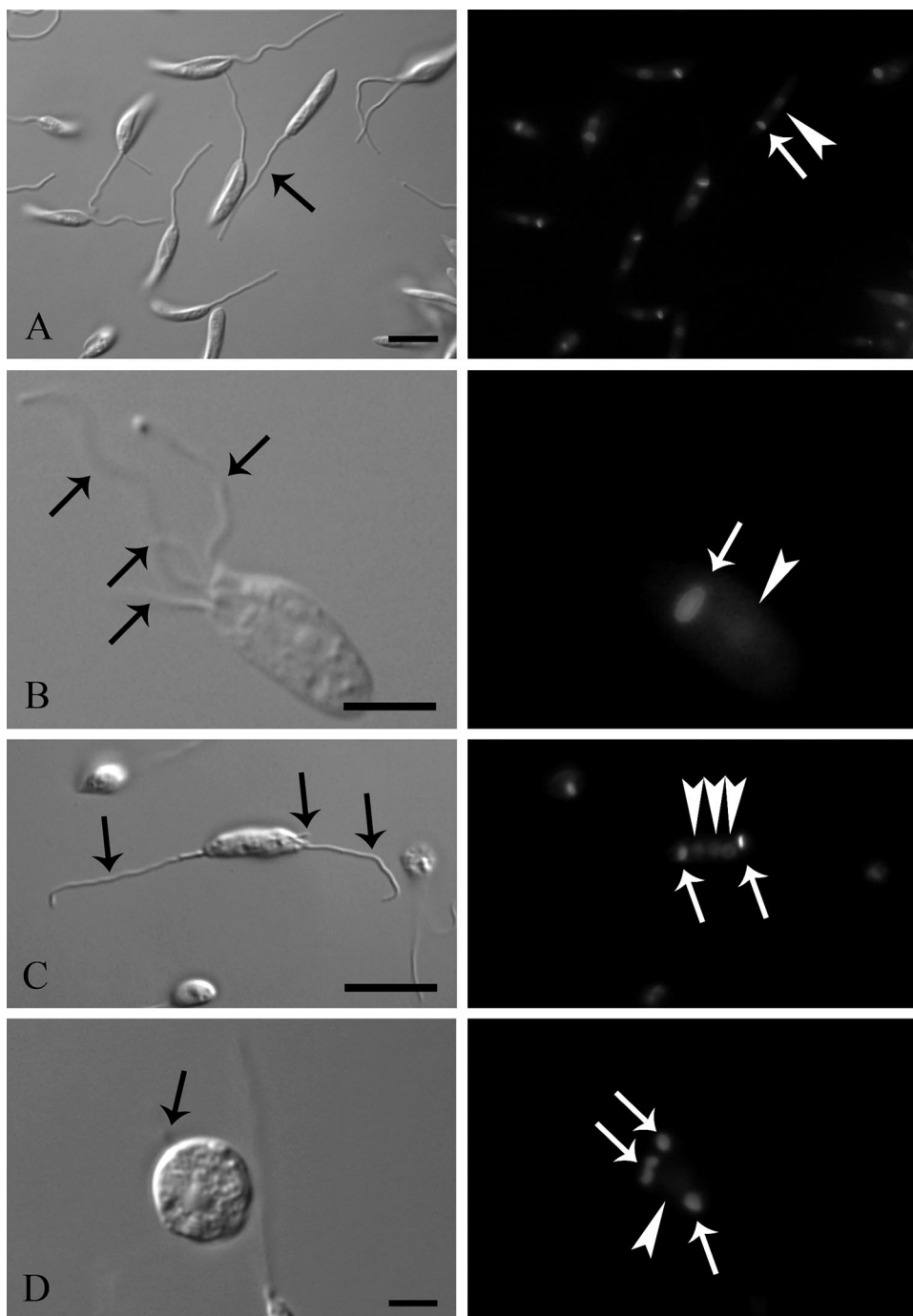


FIG. 8. DIC microscopy (left panels) and fluorescence microscopy with DAPI (right panels) of promastigote forms of *Leishmania amazonensis* control cells (A), cells treated with 50 nM ER-119884 for 24 h (B), cells treated with 10 nM ER-119884 for 48 h (C), and cells treated with 10 nM ER-119884 for 72 h (D) showing changes in the number of flagella, kinetoplasts, and nuclei. (A) General overview of control parasites presenting one flagellum (black arrow), one kinetoplast (white arrow), and one nucleus (white arrowhead); (B) after 24 h of treatment, we found parasites presenting four flagella (black arrows) but only one kinetoplast (white arrow) and one nucleus (white arrowhead); (C) after 48 h, parasites with three flagella (black arrows), two kinetoplasts (white arrow), and three nuclei (white arrowheads) were observed; (D) after 72 h, we found that the parasites had swelled and that some of them presented a variable number of flagella (black arrow), kinetoplasts (white arrows), and nuclei (white arrowhead). Bars, 5 μ m.

12A, arrowheads). In other cells, a large number of lipid droplets with various morphologies were seen (Fig. 12B to D), consistent with the accumulation of lipid droplets detected by Nile Red fluorescence. At least three different populations of lipid droplets could be identified: (i) inclusions with

a very electron-dense membrane (Fig. 12B, arrows), (ii) classical lipid inclusions completely stained with osmium tetroxide (Fig. 12C and D, arrows), and (iii) electron-lucent lipid bodies (Fig. 12D, large arrows and stars) surrounded by a typical monolayer of phospholipids (Fig. 12D). In some

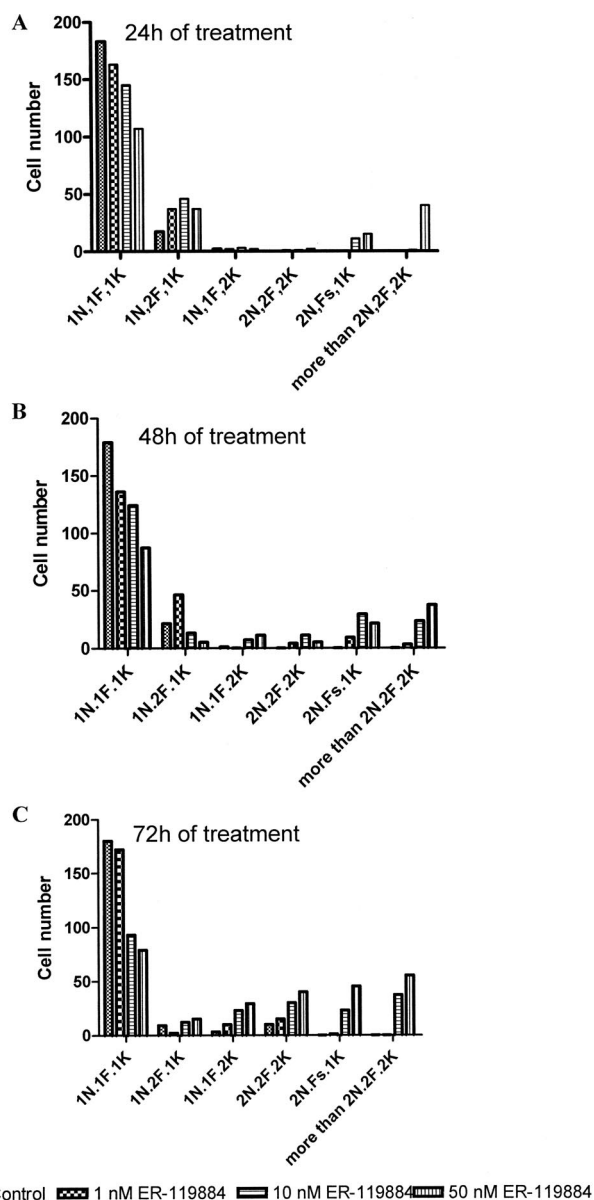


FIG. 9. Proportions of 200 cells counted with different cell division phenotypes observed until 96 h of growth and 72 h of treatment with ER-119884. (A) After 24 h of treatment; (B) after 48 h of treatment; (C) after 72 h of treatment. These analyses represent the quantification of the fluorescence with DAPI shown in Fig. 6. N, nucleus; F, flagellum; K, kinetoplast.

cases, by observation at high magnification (Fig. 12C, star), we could see lipid droplets presenting a core not stained with osmium tetroxide, which probably means a difference in the lipid composition of these structures, probably indicating the presence of saturated fatty acids.

Additional lesions observed in drug-treated parasites included the presence of promastigotes with two or more nuclei (Fig. 13A), as already described above by the use of DAPI staining; the presence of many vesicles in the flagellar pocket or in close association with it (Fig. 13B, arrowheads), sometimes resembling the structure described as the contractile vacuole (Fig. 13B, stars); and the presence of cells with a highly vacuolized cytoplasm (Fig. 13C, arrows) and nuclei in which the chromatin was drastically altered (Fig. 13D).

DISCUSSION

Quinuclidine derivatives are well-known potent inhibitors of mammalian SQS (5, 7, 33). The first quinuclidine tested against *T. cruzi* (4, 49) and *Leishmania* spp. (39, 49) was BPO-OH, which inhibited native SQS and led to cell death in association with the depletion of the parasite's endogenous sterols, demonstrating that SQS is essential for cell viability in trypanosomatids. It has also been found that other quinuclidine derivatives inhibit the *Leishmania major* recombinant SQS in the nanomolar range and induce the depletion of endogenous sterols and growth inhibition in whole parasites of the NR strain of *Leishmania amazonensis* (6, 26). The novel quinuclidine derivatives ER-119884 and E5700 against *Trypanosoma cruzi* were previously found to be particularly potent inhibitors of SQS; this inhibition led to the complete depletion of the parasite's endogenous sterols and cell death at low-nanomolar to subnanomolar concentrations (48). However, a recent study demonstrated that ER-119884 and E5700 were also potent inhibitors of the growth of *Toxoplasma gondii*, a parasite that does not code for SQS and which is incapable of the de novo biosynthesis of sterols (32), indicating that these compounds have other intracellular targets in apicomplexan parasites. The antiproliferative activities of these novel quinuclidine derivatives against *Leishmania amazonensis* observed in this study were similar to those found against *T. cruzi* (48), with IC_{50} s against both extracellular promastigotes and intracellular amastigotes in the low-nanomolar to subnanomolar range (Table 1). It must be noted that the clinically relevant intracellular amastigotes stages are significantly more susceptible than the extracellular forms for both parasites. Such high degrees of susceptibility and the lack of effects against host cells place E5700 and ER-119884 among the compounds with the most potent and selective activities against trypanosomatid parasites ever tested. This selectivity has also been demonstrated in vivo against *T. cruzi* (48) and in the present work against *L. amazonensis* in macrophage cultures, where it was shown that ER-119884 and E5700 had IC_{50} s against the host cells that were 4 to 5 orders of magnitude larger than those against the intracellular parasites (Fig. 4).

The potencies of the quinuclidine derivatives as inhibitors of purified *L. amazonensis* SQS (Table 2) are quantitatively similar to their antiproliferative effects (Table 1 and Fig. 2), suggesting a causal relationship between the two phenomena. However, the level of antiproliferative activity of ER-119884 against *L. amazonensis* promastigotes was higher than that of E5700, which is in contrast to their relative potencies against purified SQS (compare Tables 1 and 2), indicating that the first compound could have a better ability to permeate the parasite's cell membranes or that it has a second target in these cells. Support for the notion that a primary mechanism of action of these compounds is inhibition of SQS comes from the correlation between the depletion of the parasite's endogenous sterols and growth inhibition, but as noted above, full growth arrest and a loss of cell viability took place at concentrations lower than those required for complete endogenous sterol depletion (Fig. 2 and Table 4), again suggesting other mechanisms of action. In any case, the fact that both compounds act as mixed or noncompetitive SQS inhibitors (Table 3) suggests that it is unlikely that they would be displaced from the active

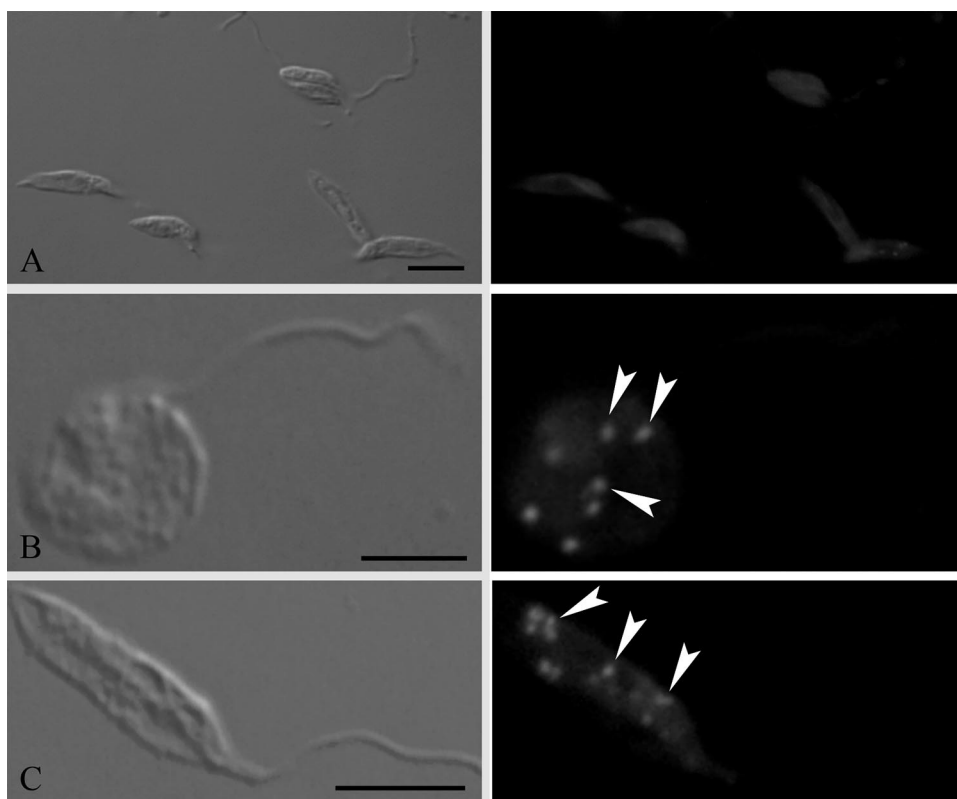


FIG. 10. DIC microscopy (left panels) and fluorescence microscopy with Nile red (right panels) of promastigote forms of *Leishmania amazonensis* control cells (A) and cells treated with 10 nM ER-119884 for 24 h (B and C) showing the presence of lipid droplets (white arrowheads) in the cytoplasm of the treated parasites. Bars, 5 μ m.

site of the enzyme as a consequence of substrate accumulation in live cells.

Conventional light microscopy, fluorescence microscopy, and transmission electron microscopy of thin sections have been used to identify the protozoan structures affected by BPQ-OH (Fig. 7) (39) and by ER-119884 and E5700 in *L. amazonensis* (this study). Since the shape of the parasite results from the spatial organization of the subpellicular microtubules whose principal component is tubulin, we decided to look for the distribution of this protein in control and drug-treated cells by immunofluorescence microscopy. Our observations showed a significant change between the labeling patterns of control cells and ER-119884- or BPQ-OH-treated cells, indicating a topological rearrangement of the protein (Fig. 7). However, the structure of the microtubules was not changed, as observed by electron microscopy (Fig. 11 to 13). Therefore, it is possible that the changes observed are not due to a direct effect of the drugs on the subpellicular microtubules but are due to an indirect effect resulting from the complete depletion of essential endogenous sterols of the plasma membrane (48, 49), which can lead to drastic modifications of its physical properties (50) and subsequently alter its association with the subpellicular microtubules (for a review, see reference 20). These changes in the plasma membrane and subpellicular microtubules were previously observed in a study on the effects of BPQ-OH in *L. amazonensis* (39) and are in agreement with the results obtained in the present study by analysis of the tubulin

distribution by an immunofluorescence assay. Another explanation would be that ER-119884 and BPQ-OH have a specific effect on some other component of the microtubular array, as the effect was not seen in E5700-treated cells. This is the first report that sterol biosynthesis inhibitors induce modifications in the cytoskeleton constituted by the subpellicular microtubules. It was recently shown in tumor mast cells that the cholesterol depletion induced by methyl- β -cyclodextrin can lead to changes in the actin cytoskeleton by the disruption of lipid rafts (15).

We also used fluorescence microscopy, in association with DIC light microscopy, to analyze the relative numbers of nuclei, kinetoplasts, and flagella in control and drug-treated cells. When DAPI was used to visualize the nucleus and the kinetoplast, marked alterations of the cell cycle were observed in a significant proportion of treated cells (Fig. 8), and these alterations increased with longer exposures to the drugs (Fig. 9). We had shown in a previous study that treatment with BPQ-OH also leads to the appearance of multinucleated parasites (39). In the present study, this effect was observed in parasites treated with ER-119884 but not in those treated with E5700, again suggesting a second target for the former compound. The effect was already evident after just 24 h of contact with the drug, when most cells were still dividing: the affected cells presented abnormal numbers of flagella, nuclei, and kinetoplasts; and the relative proportion of these abnormal cells increased with time. Again, there are two possible explanations

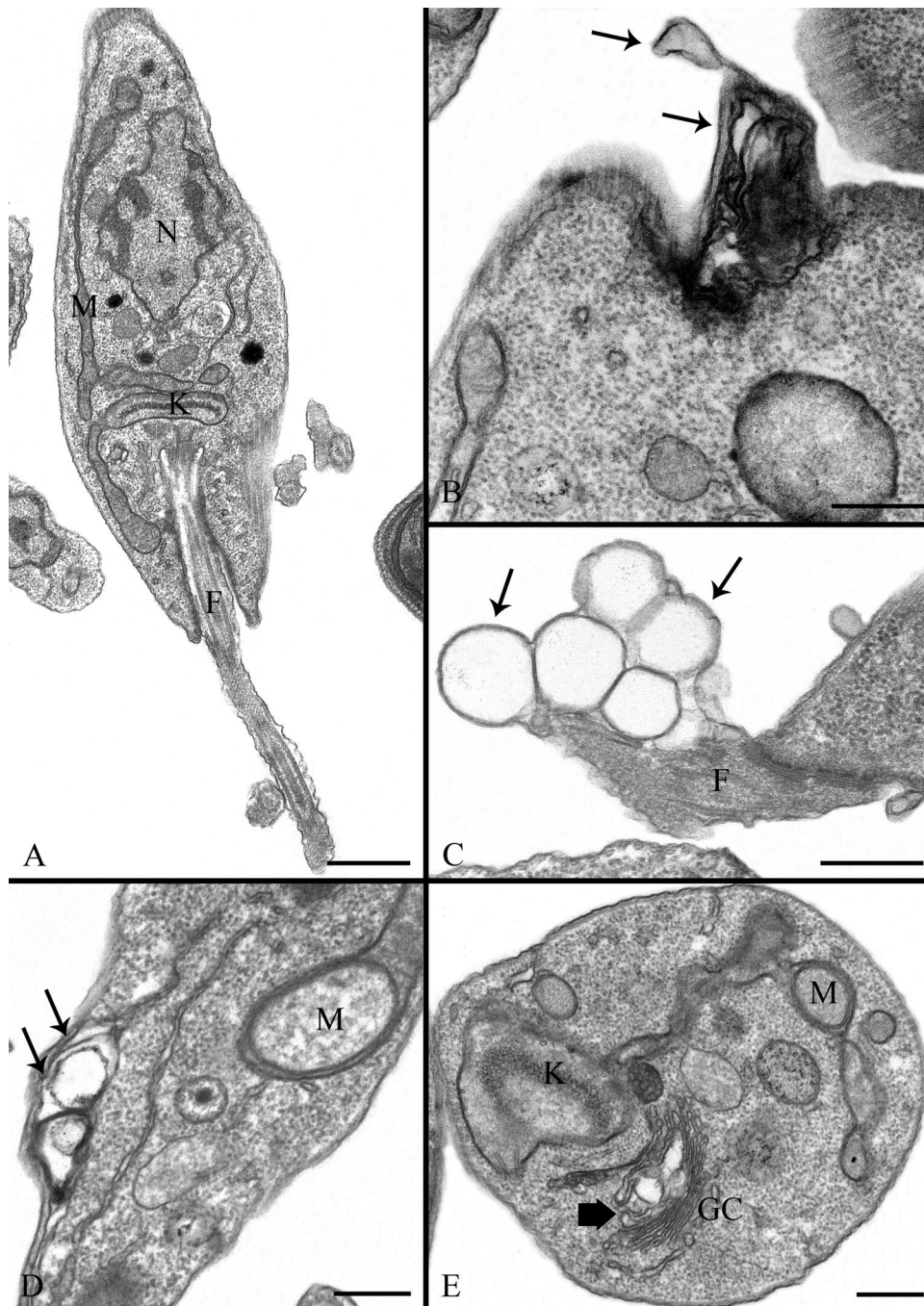


FIG. 11. Ultrathin sections of promastigote forms of *Leishmania amazonensis* control cells (A) and cells treated with 50 nM ER-119884 for 24 h (B), 1 nM E5700 for 48 h (C), 10 nM E5700 for 24 h (D), and 5 nM ER-119884 for 24 h (E). (A) General overview of a normal promastigotes presenting any alteration in the nucleus (N), flagellum (F), mitochondrion (M), and kinetoplast (K). Note that the plasma membrane and the domain that surrounds the flagellum appear to be normal. (B and C) The images indicate a dramatic lesion in the membrane that surrounds the cell body and the flagellum (arrows); (D and E) the images suggest changes in the endoplasmic reticulum (arrows) and in Golgi complex (big arrow). GC, Golgi complex; F, flagellum; K, kinetoplast; M, mitochondrion; N, nucleus. Bars, 0.5 μm .

for these effects: (i) the cells do not complete cell division due to the depletion of essential endogenous sterols, which control the dynamics of the membrane but which are also key regulators of the cell cycle (12, 16); or (ii) the organization of the cytoskeleton necessary for the completion of the cytokinesis process, which requires interactions with the plasma nuclear

membranes, is in some way specifically affected by ER-119884, as discussed above for the subpellicular microtubules.

Another prominent effect resulting from the treatment of the parasites with ER-119884 or E5700 was the accumulation of lipid droplets in the cytoplasm (Fig. 10 and 12), probably resulting from the accumulation of lipid precursors due to the

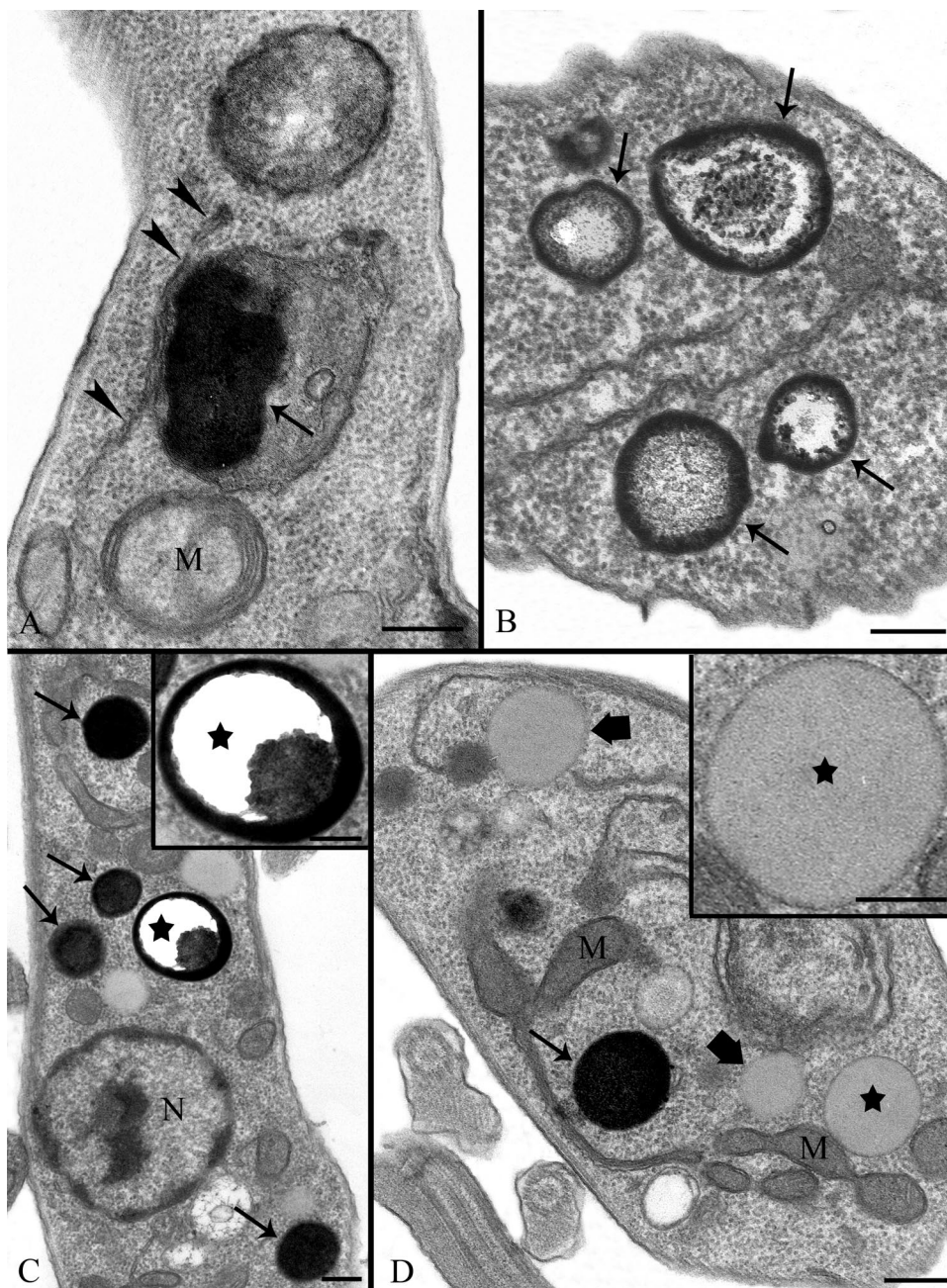


FIG. 12. Ultrathin sections of promastigote forms of *Leishmania amazonensis* treated with 5 nM ER-119884 for 48 h (A), 5 nM E5700 for 48 h (B), 10 nM ER-119884 for 72 h (C), and 10 nM ER-119884 for 48 h (D). (A) The image suggests an accumulation of lipid (arrow) in the cytoplasm, which appears to be surrounded by endoplasmic reticulum (arrowheads); (B to D) the presence of many lipid droplets in the cytoplasm with distinct morphologies. From the image in panel B, we can observe an accumulation of osmium tetroxide only in the periphery of the structures. On the other hand, the image in panel C shows the presence of electron-dense lipid inclusions (arrows), but in some cases, the lumen of these structures appear to be empty (stars). In the image in panel D, we can observe a population of lipid bodies surrounded by a monolayer (large arrows and stars) that could be better visualized under higher magnification (star), although more electron-dense inclusions (arrow) also appear. M, mitochondrion; N, nucleus. Bars, 0.5 μm (A to D) and 0.25 μm (C and D insets).

drastic alteration of the sterol content of the parasite's membranes. The lipid droplets could be identified by fluorescence microscopy of Nile Red-stained cells and by transmission electron microscopy. Each lipid droplet or lipid inclusion was surrounded by a monolayer of phospholipids, similar to those described in many eukaryotic cells (34). These structures have

a hydrophobic core usually composed of triacylglycerol, diacylglycerol, and esterified sterols (34). Quinclidine derivatives are also known to interfere with fatty acid and phospholipid biosynthesis in mammalian cells (22), and a similar phenomenon has been reported in *Chitridia deanei* cells after treatment with sterol 24-methenyltransferase inhibitors (35). Lipid inclu-

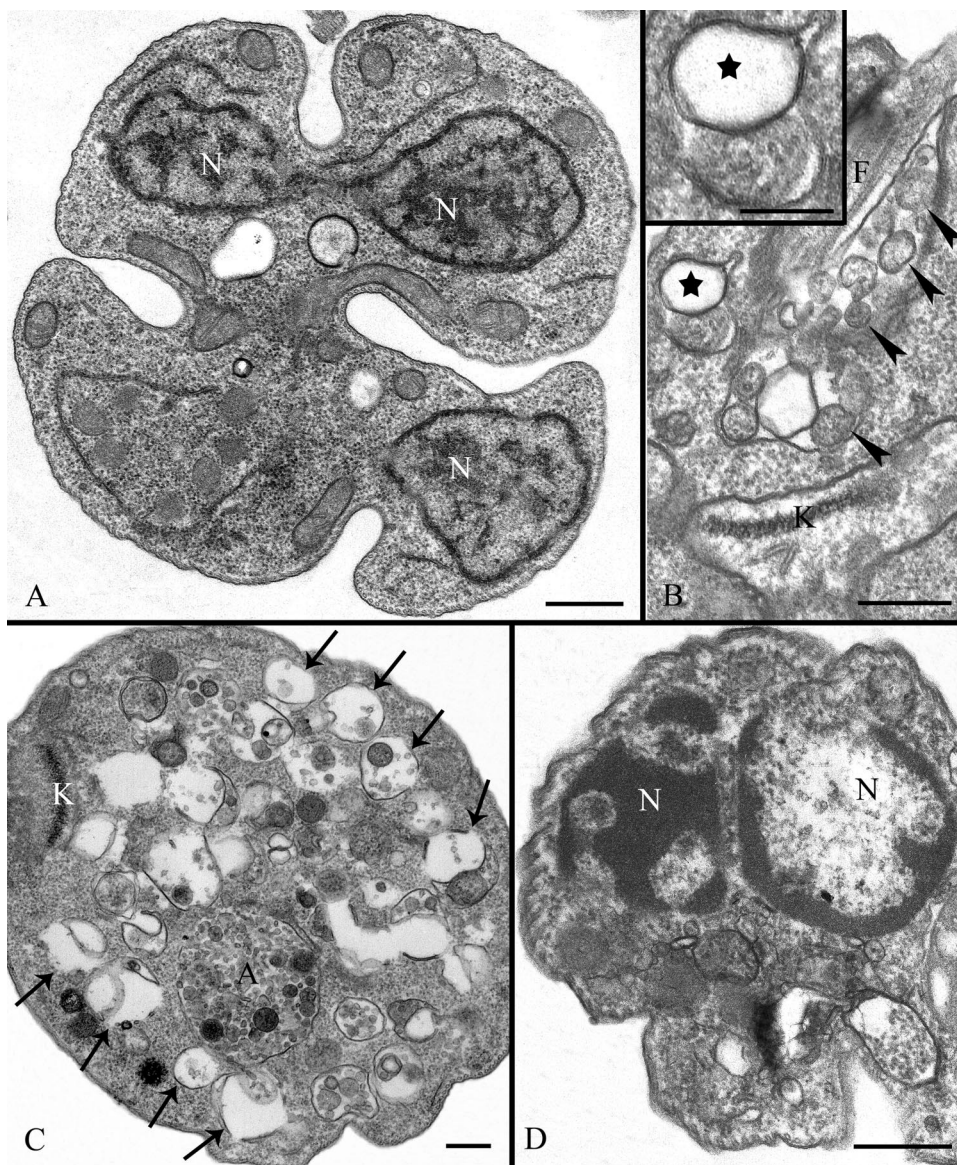


FIG. 13. Ultrathin sections of promastigote forms of *Leishmania amazonensis* treated with 50 nM ER-119884 for 96 h (A), 50 nM E5700 for 48 h (B), 50 nM ER-119884 for 72 h (C), and 50 nM ER-119884 for 96 h (D). (A) Promastigote presenting three nuclei. (B) The presence of many vesicles inside and in close association with the flagellar pocket (arrowheads). The image in panel B also shows the presence of a structure similar to the contractile vacuole in the anterior region of the parasite (stars). (C) After treatment, many parasites presented a complete vacuolization of the cytoplasm (arrows), in some cases appearing as structures similar to autophagosomes (A). (D) Some parasites also presented changes in the chromatin condensation. As observed in panel A, the cell had two nuclei. A, autophagosome; F, flagellum; K, kinetoplast; N, nucleus. Bars, 0.5 μm (panels A to D) and 0.25 μm (panel B inset).

sions were also observed in *L. major* null mutants for serine palmitoyltransferase, an enzyme involved in sphingolipid biosynthesis (54, 55), and in *T. cruzi* epimastigotes after the perturbation of sphingolipid biosynthesis (40). However, large numbers of lipid inclusions have also been reported in taxol-treated *T. cruzi* (13), indicating that lipid body formation can occur as a consequence of many different perturbations to the parasite's cellular functions.

Significant changes were also found in internal membranes, such as those of the Golgi complex and the endoplasmic reticulum (Fig. 11), indicating that sterol biosynthesis inhibition can alter these membranes. In mammalian cells, it has been shown

that the depletion of cholesterol leads to the profound alteration of the de novo synthesis of sphingolipids, indicating that this sterol is involved in the endocytic and secretory pathways, probably in association with lipid raft formation and recycling (31). The presence of vacuoles near the Golgi complex and many vesicles inside the flagellar pocket in *L. amazonensis* cells treated with the SQS inhibitors also suggest perturbations in intracellular trafficking, mainly in the secretory pathway (14, 54, 55). In addition, some electron micrographs showed changes in the flagellar pocket and the flagellar membrane, but these were not associated with the subpellicular microtubules, thus indicating that ergosterol and other 24-alkyl sterols are

essential for maintenance of the integrity of all cellular membranes in this organism.

Finally, some electron micrographs indicated that the SQS inhibitors were able to induce autophagic cell death or apoptosis processes (Fig. 13). However, more studies are necessary to better describe the cell death phenotypes after treatment with these ergosterol biosynthesis inhibitors.

In conclusion, this work found that ER-119884 and E5700 are potent inhibitors of the growth of *L. amazonensis* that induce dramatic effects on the morphology and ultrastructure of these unicellular organisms, most probably resulting from inhibition of endogenous sterol biosynthesis at the level of SQS and the resulting depletion of essential endogenous sterols. However, some of our observations indicate that the ER-119884 may also interfere with other cellular processes, such as cytoskeleton organization and cytokinesis. The remarkable potencies and selective anti-*Leishmania* activities of these compounds in vitro warrant further studies with animal models of the several forms of leishmaniasis, which are under way in our laboratories.

ACKNOWLEDGMENTS

This work was supported by the European Commission (contract ICA4-CT-2001-10074 to W.D.S. and J.A.U.), the Programa de Núcleos de Excelência, the Conselho Nacional de Desenvolvimento Científico e Tecnológico, and the Fundação Carlos Chagas Filho de Amparo à Pesquisa do Estado do Rio de Janeiro (FAPERJ). J.C.F.R. had a Ph.D. fellowship from FAPERJ.

We thank Keith Gull for kindly providing the TAT1 antibody. J.C.F.R. gratefully acknowledges Érica S. Martins-Duarte for helpful discussions.

REFERENCES

- Barral, A., D. Pedral-Sampaio, G. Grimaldi, Jr., H. Momen, D. McMahon-Pratt, A. R. de Jesus, R. Almeida, R. Badaró, M. Barral, and E. M. Carvalho. 1991. Leishmaniasis in Bahia, Brazil: evidence that *Leishmania amazonensis* produces a wide spectrum of clinical disease. *Am. J. Trop. Med. Hyg.* **44**: 536–546.
- Barrett-Bee, K., and N. Ryder. 1992. Biochemical aspects of ergosterol biosynthesis inhibition, p. 437–475. In J. Sutcliffe, and N. H. Georgopapadokou (ed.), *Emerging targets in antibacterial and antifungal chemotherapy*. Chapman & Hall, New York, NY.
- Berman, J. 2005. Recent developments in leishmaniasis: epidemiology, diagnosis, and treatment. *Curr. Infect. Dis. Rep.* **7**:33–38.
- Braga, M. V., J. A. Urbina, and W. de Souza. 2004. Effects of squalene synthase inhibitors on the growth and ultrastructure of *Trypanosoma cruzi*. *Int. J. Antimicrob. Agents* **24**:72–78.
- Brown, G. R., D. S. Clarke, A. J. Foubister, S. Freeman, P. J. Harrison, M. C. Johnson, K. B. Mallion, J. McCormick, F. McTaggart, A. C. Reid, G. J. Smith, and M. J. Taylor. 1996. Synthesis and activity of a novel series of 3-biarylquinuclidine squalene synthase inhibitors. *J. Med. Chem.* **39**:2971–2979.
- Cammerer, S., C. J. Jimenez, S. Jones, L. Gros, S. O. Lorente, C. Rodriguez, J. C. F. Rodrigues, A. Caldera, L. M. Ruiz-Pérez, W. de Souza, M. Kaiser, R. Brun, J. A. Urbina, D. Gonzalez-Pacanowska, and I. H. Gilbert. 2007. Quinuclidine derivatives as potential anti-parasitics. *Antimicrob. Agents Chemother.* **51**:4049–4061.
- Charlton-Menys, V., and P. N. Durrington. 2007. Squalene synthase inhibitors: clinical pharmacology and cholesterol-lowering potential. *Drugs* **67**: 11–16.
- Concepcion, J. L., D. Gonzalez-Pacanowska, and J. A. Urbina. 1998. 3-Hydroxy-3-methyl-glutaryl-CoA reductase in *Trypanosoma (Schizotrypanum) cruzi*: subcellular localization and kinetic properties. *Arch. Biochem. Biophys.* **352**:114–120.
- Contreras, L. M., J. Vivas, and J. A. Urbina. 1997. Altered lipid composition and enzyme activities of plasma membranes from *Trypanosoma (Schizotrypanum) cruzi* epimastigotes grown in the presence of sterol biosynthesis inhibitors. *Biochem. Pharmacol.* **53**:697–704.
- Croft, S. L., M. P. Barrett, and J. A. Urbina. 2005. Chemotherapy of trypanosomiasis and leishmaniasis. *Trends Parasitol.* **21**:508–512.
- Croft, S. L., S. Sundar, and A. H. Fairlamb. 2006. Drug resistance in leishmaniasis. *Clin. Microbiol. Rev.* **19**:111–126.
- Dahl, C. E., H.-P. Biemann, and J. S. Dahl. 1987. A protein kinase antigenically related to pp60^{src} possibly involved in yeast cell cycle control: positive *in vivo* regulation by sterol. *Proc. Natl. Acad. Sci. USA* **84**:4012–4016.
- Dantas, A. P., H. S. Barbosa, and S. L. de Castro. 2003. Biological and ultrastructural effects of the anti-microtubule agent taxol against *Trypanosoma cruzi*. *J. Submicrosc. Cytol. Pathol.* **35**:287–294.
- Denny, P. W., D. Goulding, M. A. J. Ferguson, and D. F. Smith. 2004. Sphingolipid-free *Leishmania* are defective in membrane trafficking, differentiation and infectivity. *Mol. Microbiol.* **52**:313–327.
- Frankel, D. J., J. R. Pfeiffer, Z. Surviladze, A. E. Johnson, J. M. Oliver, B. S. Wilson, and A. R. Burns. 2006. Revealing the topography of cellular membrane domains by combined atomic force microscopy/fluorescence imaging. *Biophys. J.* **90**:2404–2413.
- Gaber, R. F., D. M. Copple, B. K. Kennedy, M. Vidal, and M. Bard. 1989. The yeast gene ERG6 is required for normal membrane function but is not essential for biosynthesis of the cell-cycle sparking sterol. *Mol. Cell. Biol.* **9**:3447–3456.
- Ganguly, N. K. 2002. Oral miltefosine may revolutionize treatment of visceral leishmaniasis. The potential impact of miltefosine on visceral leishmaniasis in India. *TDR News* **98**:2.
- Gonzalez-Pacanowska, D., B. Arison, C. M. Havel, and J. A. Watson. 1988. Isopentenoid synthesis in isolated embryonic *Drosophila* cells. Farnesol catabolism and ω -oxidation. *J. Biol. Chem.* **263**:1301–1306.
- Grantham, A. C., M. V. Braga, J. C. F. Rodrigues, S. Cammerer, S. O. Lorente, I. H. Gilbert, J. A. Urbina, and W. de Souza. 2007. Alterations on the growth and ultrastructure of *Leishmania chagasi* induced by squalene synthase inhibitors. *Vet. Parasitol.* **146**:25–34.
- Gull, K. 1999. The cytoskeleton of trypanosomatid parasites. *Annu. Rev. Microbiol.* **53**:629–655.
- Hirst, S. L., and L. A. Stapley. 2000. Parasitology: the dawn of a new millennium. *Parasitol. Today* **16**:1–3.
- Hiyoshi, H., M. Yanachimachi, M. Ito, N. Yasuda, T. Okada, H. Ikuta, D. Shinmyo, K. Tanaka, N. Kurusu, I. Yoshida, S. Abe, T. Sacki, and H. Tanaka. 2003. Squalene synthase inhibitors suppress triglyceride biosynthesis through the farnesol pathway in rat hepatocytes. *J. Lipid Res.* **44**:128–135.
- Lazardi, K., J. A. Urbina, and W. de Souza. 1990. Ultrastructural alterations induced by two ergosterol biosynthesis inhibitors, ketoconazole and terbinafine, on epimastigotes and amastigotes of *Trypanosoma (Schizotrypanum) cruzi*. *Antimicrob. Agents Chemother.* **34**:2097–2105.
- Lazardi, K., J. A. Urbina, and W. de Souza. 1991. Ultrastructural alterations induced by ICI 195,739, a bis-triazole derivative with strong antiproliferative action against *Trypanosoma (Schizotrypanum) cruzi*. *Antimicrob. Agents Chemother.* **35**:736–740.
- Liendo, A., G. Visbal, M. M. Piras, R. Piras, and J. A. Urbina. 1999. Sterol composition and biosynthesis in *Trypanosoma cruzi* amastigotes. *Mol. Biochem. Parasitol.* **104**:81–91.
- Lorente, S. O., R. Gomez, C. J. Jimenez, S. Cammerer, V. Yardley, K. de Luca-Fradley, S. L. Croft, L. M. Ruiz-Perez, J. A. Urbina, D. Gonzalez-Pacanowska, and I. H. Gilbert. 2005. Biphenylquinuclidines as inhibitors of squalene synthase and growth of parasitic protozoa. *Bioorg. Med. Chem.* **13**:3519–3529.
- Lorente, S. O., J. C. F. Rodrigues, C. J. Jimenez, M. Joyce-Menekse, C. Rodriguez, S. L. Croft, V. Yardley, K. de Luca-Fradley, L. M. Ruiz-Perez, J. A. Urbina, W. de Souza, D. Gonzalez-Pacanowska, and I. H. Gilbert. 2004. Novel azasterols as potential agents for treatment of leishmaniasis and trypanosomiasis. *Antimicrob. Agents Chemother.* **48**:2937–2950.
- Luis, L., A. Ramirez, C. M. Aguilar, S. Eresh, D. C. Barker, and A. Mendoza-Leon. 1998. The genomic fingerprint of the coding region of the beta-tubulin in *Leishmania* identification. *Acta Trop.* **69**:310–316.
- Magaraci, F., C. C. Jimenez, C. Rodriguez, J. C. F. Rodrigues, M. V. Braga, V. Yardley, K. de Luca-Fradley, L. M. Ruiz-Perez, J. A. Urbina, W. de Souza, D. Gonzalez-Pacanowska, and I. H. Gilbert. 2003. Azasterols as inhibitors of sterol 24-methyltransferase in *Leishmania* species and *Trypanosoma cruzi*. *J. Med. Chem.* **46**:4714–4727.
- Marsden, P. D., and T. C. Jones. 1985. Clinical manifestations, diagnosis and treatment of leishmaniasis, p. 183–198. In K. P. Chang and R. S. Bray (ed.), *Human parasitic diseases, leishmaniasis*, vol. 1. Elsevier Science Publishers, New York, NY.
- Martin, O. C., M. E. Comly, E. J. Blanchette-Mackie, P. G. Pentchev, and R. E. Pagano. 1993. Cholesterol deprivation affects fluorescence properties of a ceramide analog at the Golgi apparatus of living cells. *Proc. Natl. Acad. Sci. USA* **90**:1661–1665.
- Martins-Duarte, E. S., J. A. Urbina, W. de Souza, and R. C. Vommaro. 2006. Antiproliferative activities of two novel quinuclidine inhibitors against *Toxoplasma gondii* tachyzoites *in vivo*. *J. Antimicrob. Chemother.* **58**:59–65.
- McTaggart, F., G. R. Brown, R. G. Davidson, S. Freeman, G. A. Holdgate, K. B. Mallion, D. J. Mirrlees, G. J. Smith, and W. H. Ward. 1996. Inhibition of squalene synthase of rat liver by novel 3'-substituted quinuclidines. *Biochem. Pharmacol.* **51**:1477–1487.
- Murphy, D. J. 2001. The biogenesis and functions of lipid bodies in animals, plants and microorganisms. *Prog. Lipid Res.* **40**:325–438.
- Palmié-Peixoto, I., M. R. Rocha, J. A. Urbina, W. de Souza, M. Einicker-

- Lamas, and M. C. M. Motta. 2006. Effects of sterol biosynthesis inhibitors on endosymbiont-bearing trypanosomatids. *FEMS Microbiol. Lett.* **255**:33–42.
36. Roberts, C. W., R. McLeod, D. W. Rice, M. Ginger, M. L. Chance, and L. J. Goad. 2003. Fatty acid and sterol metabolism: potential antimicrobial targets in apicomplexan and trypanosomatid parasitic protozoa. *Mol. Biochem. Parasitol.* **126**:129–142.
 37. Rodrigues, J. C. F., C. F. Bernardes, G. Visbal, J. A. Urbina, A. E. Vercesi, and W. de Souza. 2007. Sterol methenyl transferase inhibitors alter the ultrastructure and function of the *Leishmania amazonensis* mitochondrion leading to potent growth inhibition. *Protist* **158**:447–456.
 38. Rodrigues, J. C. F., M. Attias, C. Rodriguez, J. A. Urbina, and W. de Souza. 2002. Ultrastructural and biochemical alterations induced by 22,26-azasterol, a $\Delta^{24(25)}$ -sterol methyltransferase inhibitors, on promastigote and amastigote forms of *Leishmania amazonensis*. *Antimicrob. Agents Chemother.* **46**:487–499.
 39. Rodrigues, J. C. F., J. A. Urbina, and W. de Souza. 2005. Antiproliferative and ultrastructural effects of BPO-OH, a specific inhibitor of squalene synthase, on *Leishmania amazonensis*. *Exp. Parasitol.* **111**:230–238.
 40. Salto, M. L., L. E. Bertello, M. Vieira, R. Docampo, S. N. Moreno, and R. M. Lederkremer. 2003. Formation and remodeling of inositolphosphoceramide during differentiation of *Trypanosoma cruzi* form trypomastigote to amastigote. *Eukaryot. Cell* **2**:756–768.
 41. Sealey-Cardona, M., S. Cammerer, S. Jones, L. M. Ruiz-Pérez, R. Brun, I. H. Gilbert, J. A. Urbina, and D. González-Pacanoska. 2007. Kinetic characterization of squalene synthase from *Trypanosoma cruzi*: selective inhibition by quinuclidine derivatives. *Antimicrob. Agents Chemother.* **51**:2123–2129.
 42. Sinderman, H., S. L. Croft, K. R. Engel, W. Bommer, H. J. Eibl, C. Unger, and J. Engel. 2004. Miltefosine (Impavido): the first oral treatment against leishmaniasis. *Med. Microbiol. Immunol.* **193**:173–180.
 43. Tait, R. M. 1992. Development of a radiometric spot-wash assay for squalene synthase. *Anal. Biochem.* **203**:310–316.
 44. Urbina, J. A., C. E. Osorno, and A. Rojas. 1990. Inhibition of phosphoenol pyruvate carboxykinase from *Trypanosoma (Schizotrypanum) cruzi* epimastigotes by 3-mercaptopycolinic acid: *in vitro* and *in vivo* studies. *Arch. Biochem. Biophys.* **282**:91–99.
 45. Urbina, J. A., G. Payares, C. Sanoja, J. Molina, R. Lira, Z. Brener, and A. J. Romanha. 2003. Parasitological cure of acute and chronic experimental Chagas disease using the long-acting experimental triazole TAK-187. Activity against drug-resistant *Trypanosoma cruzi* strains. *Int. J. Antimicrob. Agents* **21**:39–48.
 46. Urbina, J. A., G. Payares, C. Sanoja, R. Lira, and A. J. Romanha. 2003. *In vitro* and *in vivo* activities of ravuconazole on *Trypanosoma cruzi*, the causative agent of Chagas disease. *Int. J. Antimicrob. Agents* **21**:27–38.
 47. Urbina, J. A. 1997. Lipid biosynthesis pathways as chemotherapeutic targets in kinetoplastid parasites. *Parasitology* **114**:S91–S99.
 48. Urbina, J. A., J. L. Concepcion, A. Caldera, G. Payares, C. Sanoja, T. Otomo, and H. Hiyoshi. 2004. *In vitro* and *in vivo* activities of ES700 and ER-119884, two novel orally active squalene synthase inhibitors, against *Trypanosoma cruzi*. *Antimicrob. Agents Chemother.* **48**:2379–2387.
 49. Urbina, J. A., J. L. Concepcion, S. Rangel, G. Visbal, and R. Lira. 2002. Squalene synthase as a chemotherapeutic target in *Trypanosoma cruzi* and *Leishmania amazonensis*. *Mol. Biochem. Parasitol.* **125**:35–45.
 50. Urbina, J. A., S. Pekerar, H. B. Le, J. Patterson, B. Montez, and E. Oldfield. 1995. Molecular order and dynamics of phosphatidylcholine bilayer membranes in the presence of cholesterol, ergosterol and lanosterol—a comparative study using ^2H , ^{13}C and ^{31}P NMR spectroscopy. *Biochim. Biophys. Acta* **1238**:163–176.
 51. Urbina, J. A., J. Vivas, K. Lazard, J. Molina, G. Payares, M. M. Piras, and R. Piras. 1996. Antiproliferative effects of $\Delta^{24(25)}$ -sterol methyltransferase inhibitors on *Trypanosoma (Schizotrypanum) cruzi*: *in vitro* and *in vivo* studies. *Chemotherapy* **42**:294–307.
 52. Vivas, J., J. A. Urbina, and W. de Souza. 1996. Ultrastructural alterations in *Trypanosoma (Schizotrypanum) cruzi* induced by $\Delta^{24(25)}$ -sterol methyltransferase inhibitors and their combinations with ketoconazole. *Int. J. Antimicrob. Agents* **7**:235–240.
 53. WHO. 1990. Control of the leishmaniasis. Report of a WHO expert committee. W. H. O. Tech. Rep. Ser. **793**:1–158.
 54. Zhang, K., F.-F. Hsu, D. A. Scott, R. Docampo, J. Turk, and S. M. Beverley. 2005. *Leishmania* salvage and remodeling of host sphingolipids in amastigote survival and acidocalcisome biogenesis. *Mol. Microbiol.* **55**:1566–1578.
 55. Zhang, K., M. Showalter, J. Revollo, F.-F. Hsu, J. Turk, and S. M. Beverley. 2003. Sphingolipids are essential for differentiation but not growth in *Leishmania*. *EMBO J.* **22**:6016–6026.